OPEN

Enhancing Efficacy of TCR-engineered CD4+ T Cells Via Coexpression of CD8α

Victoria E. Anderson, Sara S. Brilha, Anika M. Weber, Annette Pachnio, Guy E. Wiedermann, Sumaya Dauleh, Tina Ahmed, George R. Pope, Laura L. Quinn, Roslin Y. Docta, Adriano Quattrini, Siobhan Masters, Neil Cartwright, Preetha Viswanathan, Luca Melchiori, Louise V. Rice, Alexandra Sevko, Claire Gueguen, Manoj Saini, Barbara Tavano, Rachel J.M. Abbott, Jonathan D. Silk, Bruno Laugel, Joseph P. Sanderson, and Andrew B. Gerry

Summary: Adoptive cell therapy with T cells expressing affinity-enhanced T-cell receptors (TCRs) is a promising treatment for solid tumors. Efforts are ongoing to further engineer these T cells to increase the depth and durability of clinical responses and broaden efficacy toward additional indications. In the present study, we investigated one such approach: T cells were transduced with a lentiviral vector to coexpress an affinity-enhanced HLA class I–restricted TCR directed against MAGE-A4 alongside a CD8α coreceptor. We hypothesized that this approach would enhance CD4+ T-cell helper and effector functions, possibly leading to a more potent antitumor response. Activation of transduced CD4+ T cells was measured by detecting CD40 ligand expression on the surface and cytokine and chemokine secretion from CD4+ T cells and dendritic cells cultured with melanoma-associated antigen A4+ tumor cells. In addition, T-cell cytotoxic activity against 3-dimensional tumor spheroids was measured. Our data demonstrated that CD4+ T cells coexpressing the TCR and CD8α coreceptor displayed enhanced responses, including CD40 ligand expression, interferon-gamma secretion, and cytotoxic activity, along with improved dendritic cell activation. Therefore, our study supports the addition of the CD8α coreceptor to HLA class I–restricted TCR-engineered T cells to enhance CD4+ T-cell functions, which may potentially improve the depth and durability of antitumor responses in patients.

Key Words: adoptive T-cell therapy, cancer, MAGE-A4, T-cell receptor

(*J Immunother* 2023;00:000–000)

T cells engineered to express affinity-enhanced T-cell receptors (TCRs) against cancer antigens are a promising therapy, particularly against solid tumors, where chimeric antigen receptor T cells have, to date, shown limited activity.[1] Antitumor responses have been demonstrated clinically in metastatic synovial sarcoma, melanoma,[2–5] and multiple myeloma.[6] Despite demonstrated activity against solid tumors, T cells transduced with affinity-enhanced TCRs may benefit from additional engineering to promote more potent and durable responses in a broader range of cancer indications.

During antitumor immune responses, cytotoxic activity is mostly a property of CD8+ T cells. However, CD4+ T cells also play a critical role in response generation and maintenance.[7–9] Although CD4+ T cells are capable of directly inducing tumor cell death via major histocompatibility complex (MHC) class II recognition of melanoma,[10–12] CD4+ T cells are also required for the clearance of class II–negative tumors, through complex interactions with professional antigen-presenting cells (APCs).[13] CD4+ T-cell function has demonstrated importance in immunotherapy response, including checkpoint inhibitors[14,15] and cancer vaccines.[16,17] Following activation by APCs, CD4+ T cells promote licensing of APCs through CD40 ligand (CD40L)/CD40 interactions and cross-activation of CD8+ T cells. In addition, activated CD4+ T cells secrete cytokines involved in immune-cell recruitment and tumor infiltration, enhancing the response and creating the antigen/epitope spreading potential.[7,18] CD4+ helper functions are also involved in forming a memory subset of CD8+ T cells and threshold lowering for CD8+ T-cell priming.[9,19,20]

Initial T-cell activation depends on TCR interactions with peptide-loaded major histocompatibility complex (pMHC) and is influenced by CD8 and CD4 coreceptors binding to MHC class I and II molecules, respectively.[21] Specifically, the CD8 complex is a heterodimer comprising CD8α and CD8β subunits.[21] CD8α binds to constant regions on MHC class I

Received for publication October 25, 2022; accepted January 12, 2023.
From Adaptimmune, Abingdon, Oxfordshire, UK.
L.M. was responsible for the concept design. L.V.R., R.Y.D, C.G., A.S., J.D.S., and B.L. developed the initial proof-of-concept studies. V.E.A and A.B.G. oversaw the project. N.C. and P.V. produced the engineered T cells. A.M.W., A.P., G.E.W., T.A., S.D., G.R.P., L.L.Q., R.Y.D., A.Q., S.M., V.E.A., B.T., R.J.M.A., M.S., and J.P.S. were responsible for the experimental design, execution of assays, and data acquisition. A.M.W., A.P., G.E.W., T.A., S.D., G.R.P., L.L.Q., V.E.A., B.T., R.J.M.A., M.S., and J.P.S. analyzed and interpreted the data. V.E.A., S.S.B., L.M., R.J.M.A., J.D.S., and A.S. drafted the manuscript. S.S.B. produced the artwork. All authors, except for L.V.R., reviewed the manuscript and approved the final version for publication.
Adaptimmune has filed patent protection on the composition of matter of the T-cell therapies used in this study (WO 2017/174824 and WO 2020/109616).
Reprints: Victoria E. Anderson, Adaptimmune, 60 Jubilee Avenue, Milton, Abingdon, Oxfordshire OX14 4RX, UK (e-mail: victoria.anderson@adaptimmune.com).
Supplemental Digital Content is available for this article. Direct URL citations appear in the printed text and are provided in the HTML and PDF versions of this article on the journal's website, www.immunotherapy-journal.com.

TABLE 1. Summary of T-Cell Batches Used in This Study

			%Vα24$^+$ of CD3$^+$ lymphocytes (%TCR$^+$)			%CD8α$^+$ of CD4$^+$ Vα24$^+$		
Batch	**Used in figures**	**HLA-A*02:01 status**	**ntd**	**ADP-A2M4**	**ADP-A2M4CD8**	**ntd**	**ADP-A2M4**	**ADP-A2M4CD8**
Large scale								
L213	1, 2, 4, S1, S7	+	0.94	64.3	59	0	0.9	97.8
L214	1, 4, S1, S4, S7	−	0.7	60.4	55	0	0	98.7
L215	1, 4, 5, S1, S4, S7	−	0.8	44.4	44.1	0	2.89	98
L216	1, 3–5, S1, S4, S6, S7	+	0.62	54.7	56.9	0	0	98.3
L217	1–5, S1, S4, S6, S7	+	0.94	57.1	61.2	0	0	99
Small scale								
SS1	3, S6	+	0.76	54.8	58.3	0	0	98.6
SS2	3, S6	+	1.04	45.3	44.9	0	0.24	98.1
SS3	2	+	0.79	52.6	50.1	0.64	0.012	98.6
SS4	2	+	0.95	42.9	46.9	0	0.11	98.3

Small-scale and large-scale T-cell batches used in the study. Each batch was manufactured from a different healthy donor. HLA-A*02:01 status, TCR transduction efficiency (%Vα24), and expression of CD8α within CD4$^+$ Vα24$^+$ population of T cells are also described for each product.
ntd, nontransduced; S, Supplemental; TCR, T-cell receptor.

molecules,[22,23] stabilizing the TCR-pMHC interaction and enhancing TCR-mediated T-cell activation.[24] CD8α contributes to T-cell activation by targeted delivery of the Src family kinase p56^{lck} to the TCR complex, enhancing CD3 phosphorylation and signal transduction.[25]

Transduction of affinity-enhanced MHC class I–restricted engineered TCRs into patient T cells generates CD8$^+$ and CD4$^+$ T cells with specificity for the same epitope, potentially bypassing the need for a complementary MHC class II–restricted antigen response. However, the lack of CD8 coreceptors on CD4$^+$ T cells can result in weak or minimal CD4$^+$ T-cell activation through the introduced MHC class I–restricted TCR.[26] Expressing the CD8 coreceptor in CD4$^+$ T cells may improve the activation and signaling of the TCR-engineered CD4$^+$ T-cell population, potentially enhancing the positive feedback loop between helper and cytotoxic subsets and providing pronounced, durable tumor clearance.

We investigated this next-generation approach by coexpressing CD8α alongside our HLA-A*02-restricted TCR,[27] which is specific to the melanoma-associated antigen A4 (MAGE-A4). ADP-A2M4 specific peptide enhanced affinity receptor (SPEAR) T cells, which express this TCR, are already in clinical trials (NCT03132922 and NCT04044768). We hypothesized that expression of CD8α in CD4$^+$ T cells alongside the ADP-A2M4 TCR (ADP-A2M4CD8) would enhance the activation of CD4$^+$ T cells in response to the HLA class I–restricted MAGE-A4–derived epitope, resulting in increased helper and effector functions, possibly leading to more potent antitumor responses. To test this hypothesis, several in vitro models were used to assess different aspects of antitumor response: T-cell activation, interaction with APCs, cytokine secretion, and killing of 3-dimensional (3D) tumor spheroids.

MATERIALS AND METHODS

Production of TCR-engineered T Cells

After obtaining informed consent, healthy donor T cells were used to produce large-scale or small-scale engineered T-cell batches. The study was approved by the South Central—Oxford A Research Ethics Committee (13/SC/0227). All methods were performed in accordance with relevant guidelines and regulations, and all mandatory laboratory health and safety procedures were complied with during the experimental work.

SPEAR T cells were engineered from isolated CD3$^+$ cells, activated using CD3/CD28 antibody-coated micro-beads (Thermo Fisher Scientific) in the presence of interleukin (IL)-2, and transduced with lentiviral particles encoding either ADP-A2M4 (affinity-enhanced TCR) or ADP-A2M4CD8 (affinity-enhanced TCR and CD8α) at a multiplicity of infection of one. They were expanded in the Xuri Cell Expansion System (GE Healthcare). T cells from each donor that were not infected with lentiviral particles were produced as nontransduced (ntd) T-cell controls. For small-scale T-cell production, CD14-depleted peripheral blood lymphocytes were transduced and expanded in 48-well or 24-well plates.

Following harvest, T cells were counted and initial transduction efficiency was determined by flow cytometry with an anti-TCR Vα24 antibody (IM2283, Beckman Coulter). Purified CD8$^+$ and CD4$^+$ populations were obtained by negative selection with either CD8β antibody (clone 3TU9618; Creative Diagnostics) and anti-mouse immunoglobulin G beads or anti-CD4$^+$ microbeads (130-048-401 or 130-045-101, respectively; Miltenyi Biotec), according to the manufacturer's instructions. Transduction efficiencies of large-scale and small-scale T-cell batches, as well as CD8α transduction in the CD4$^+$ population, are shown in Table 1. Analyses of transduced protein surface expression and percentage of CD4$^+$ versus CD8$^+$ cells at harvest are detailed in Supplemental Figure 1 (Supplemental Digital Content 1, http://links.lww.com/JIT/A706).

Tumor and Primary Cell Lines

All target cell lines used (Table 2; Supplemental Tables 1, 2, Supplemental Digital Content 1, http://links.lww.com/JIT/A706) were screened for mycoplasma contamination, and authenticity and purity were confirmed by short tandem repeat analysis and regular quantitative polymerase chain reaction to confirm expression level of MAGE-A4. Cell lines expressing copepod green fluorescent protein (GFP) or nuclear GFP were lentivirally transduced and maintained under puromycin selection.

Assessment of CD40L Surface Expression Following Stimulation

Surface expression of CD40L was analyzed on T cells following overnight stimulation. A375 (MAGE-A4$^+$) or

TABLE 2. Target Cell Lines Used in This Study, With HLA-A*02 Status and Representative Quantitative Polymerase Chain Reaction Data for MAGE-A4

Cell line	Tumor type	Used in figures	HLA-A*02:01 status	MAGE-A4 expression	MAGE-A4 status
A375	Malignant melanoma	1, 3, 5, S4, S6	+	1,205,221	+
A375.nucGFP	Malignant melanoma	2	+	1,362,527	+
A375.CopGFP	Malignant melanoma	4, S7	+	729,070	+
Nalm6	Acute lymphoblastic leukemia	3, 5, S6	+	17	−
Nalm6.nucGFP	Acute lymphoblastic leukemia	2	+	12	−
NCI-H1755	Non–small cell lung carcinoma	3, S6	+	2,123,084	+
Colo205	Colorectal carcinoma	1, S4	+	8	−

MAGE-A4 expression is presented as normalized transcript number per 10^6 reference gene transcripts.
MAGE-A4 indicates melanoma-associated antigen A4; S, Supplemental.

Colo205 (MAGE-A4$^-$) cell lines were seeded into a 96-well flat-bottom plate and left to adhere overnight at 37°C and 5% CO_2. The following day, T cells were added at an effector:target cell ratio of 5:1, and an anti-CD40L BV421 antibody (clone TRAP1; BD Horizon) was added to each well. Simultaneously, GolgiStop (BD Biosciences) was added to stabilize CD40L-antibody complexes on the cell surface. Cocultures were incubated at 37°C and 5% CO_2 for 20 hours before staining with CD3-FITC (clone SK7; Thermo Fisher Scientific), CD4-BV650 (clone SK3, BD Horizon), CD8-APCeF780 (clone SK1; Thermo Fisher Scientific), TCR Vα24-PE (clone C15, IM2283; Beckman Coulter), and LIVE/DEAD Fixable Aqua Dead Cell Stain kit (Thermo Fisher Scientific) to allow identification of specific cell subsets. Data were acquired on BD LSRFortessa X-20 instruments (BD Biosciences), using software FACSDiva, version 8.0.1 (BD Biosciences), and analyzed using FlowJo, v10.4.1 (BD Biosciences). The gating strategy is shown in Supplemental Figure 2 (Supplemental Digital Content 1, http://links.lww.com/JIT/A706).

Proliferation Assay

T-cell proliferation was assessed using Violet Proliferation Dye (VPD) 450 (BD Horizon). Ntd, ADP-A2M4, and ADP-A2M4CD8 large-scale T-cell products from 4 donors were thawed, rested for 26 hours in tryptophan-free RPMI medium (PAN-Biotech), then stained with VPD450 and incubated alone or in coculture with irradiated MAGE-A4$^+$ (A375) or MAGE-A4$^-$ (Colo205) tumor cell lines at a 5:1 effector:target ratio. T cells cultured alone or in the presence of tumor cell lines pulsed with peptide served as negative and positive controls, respectively. Following 3 days of coculture, cells were harvested and stained for T-cell markers: CD3-FITC (clone SK7; Thermo Fisher Scientific), CD4-BV605 (clone RPA-T4, BioLegend), CD8-APCeF780, and TCR Vα24-PE for TCR$^+$ cells and viability (7AAD; BD Pharmingen). Samples were acquired on the BD LSRFortessa X-20, using the BD High Throughput Sampler system (BD Biosciences). Data were acquired with FACSDiva, version 8.0.1 (gating strategy shown in Supplemental Fig. 3, Supplemental Digital Content 1, http://links.lww.com/JIT/A706), and subsequent analysis was performed using FlowJo, v10.4.1 to determine the proliferation index (Supplemental Fig. 4, Supplemental Digital Content 1, http://links.lww.com/JIT/A706).

The proliferation index corresponds to the mean number of divisions for the responding cells and was calculated based on peak VPD reductions using statistics provided by FlowJo.[28]

Monocyte-derived Dendritic Cells (DCs)

DCs were differentiated from CD14$^+$ monocytes isolated from peripheral blood mononuclear cells of healthy HLA-A*02:01 volunteers using CD14 microbeads (Miltenyi Biotec). CD14$^+$ cells were seeded at 5×10^5 cells/mL in phenol red- and HEPES-free RPMI 1640 medium supplemented with 10% fetal bovine serum, 1000 U/mL human granulocyte-macrophage colony-stimulating factor (GM-CSF), and 500 U/mL human IL-4 (differentiation medium). Every 2–3 days, half the culture medium was replaced with fresh differentiation medium. DCs were used after 7 days of differentiation.

DC Coculture Assays

For coculture assays, DCs were washed 3 times and 1×10^5 DCs seeded into 48-well plates for coculture with an equal number of MAGE-A4$^+$ (A375, NCI-H1755) or MAGE-A4$^-$ (Nalm6) target cells. Ntd, ADP-A2M4, or ADP-A2M4CD8 T cells (4×10^5) were added, and cocultures were incubated at 37°C and 5% CO_2. Additional wells of DCs alone were treated with either lipopolysaccharide or a cytokine cocktail [100 μg/mL IL-4, 100 μg/mL GM-CSF, 100 μg/mL IL-6, 1×10^8 U/mL IL-1β, 100 μg/mL prostaglandin E2, 2×10^6 U/mL tumor necrosis factor α (TNF-α)]. After 48 hours, supernatants were collected and frozen at −80°C for subsequent cytokine and chemokine analysis, or cells were harvested for analysis by flow cytometry.

To confirm DC maturation in cocultures, multicolor immunophenotypic analysis was performed by flow cytometry using BD LSRFortessa X-20 and FACSDiva software, v8.0.1. The monoclonal antibodies used were directed against CD1a-AF700 (clone HI149; BioLegend), CD14-BUV395 (clone M5E2; BD Biosciences), CD40-BV605 (clone 5C3; BioLegend), and CD80-APC (clone 2D10; BioLegend). Analysis was carried out using FlowJo v10.4.1. The gating strategy for CD80 and CD40 expression by DCs is shown in Supplemental Figure 5 (Supplemental Digital Content 1, http://links.lww.com/JIT/A706).

Cytokine and Chemokine Analysis

Cytokine and chemokine analysis in culture supernatants was performed using Bio-Plex MAGPIX (Bio-Rad Laboratories) with a 25-plex human cytokine panel (Life Technologies) according to manufacturer recommendations. Samples were acquired using a Bio-Plex MAGPIX Reader (Bio-Rad Laboratories). Preselected analytes included GM-CSF, interferon-gamma (IFN-γ), IL-2, IL-2R, IL-4, IL-5, IL-6, IL-10, IL-12 (p40/p70), IL-13, IL-17, monokine induced by interferon gamma (MIG, also known as chemokine ligand 9), macrophage inflammatory protein-1β, and TNF-α.

T-Cell Cytotoxic Activity Against 3D Tumor Spheroids

MAGE-A4$^-$ and HLA-A*02$^+$ GFP-labeled A375 melanoma cells (150 or 1200 cells/well) were seeded in PrimeSurface ultra-low-attachment 384-well microplates (S-BIO) to enable microtissue formation. Following stable spheroid formation of ~600 μm ("small") or ~800 μm ("large") diameter at 145–147 hours, either ntd, ADP-A2M4, or ADP-A2M4CD8 CD4$^+$ (80,000 cells/well), CD8$^+$ (20,000 cells/well), or unseparated (20,000 cells/well) T cells were added. Images were acquired at 3-hour intervals from the point of cell seeding until assay completion using the IncuCyte ZOOM (Sartorius) with a ×10 objective. Uniform microtissue formation was confirmed in each well before T-cell addition. Raw images of green fluorescence for all time points were exported and analyzed using a custom macro in the AxioVision software, v4.9.1 (Zeiss) to calculate the microtissue area in each well. All data were normalized to the time of T-cell addition to compensate for any small variances in microtissue size between replicates. Data for microtissue area and area under the curve were plotted up to the endpoint of the assays. Supernatants were collected from duplicate assay plates at ~48–50 hours after T-cell addition and were used to measure IFN-γ and granzyme B (GzB) secretion using enzyme-linked immunosorbent assay (ELISA) (human IFN-γ DuoSet and human GzB DuoSet; R&D Systems) with the use of a luminescent horseradish peroxidase substrate (Glo Substrate; R&D Systems). Luminescence was measured using the FLUOstar Omega plate reader (BMG Labtech).

IFN-γ Cell ELISA

Target cells, T cells, and peptide (if relevant) were added to 384-well plates precoated overnight with IFN-γ capture antibody and incubated for 48 hours. After removal of the liquid, plates were processed per supernatant ELISA. Target cells are listed in Supplemental Tables 1, 2 (Supplemental Digital Content 1, http://links.lww.com/JIT/A706) and peptides used are listed in Supplemental Table 3 (Supplemental Digital Content 1, http://links.lww.com/JIT/A706).

Data Analysis

Data were plotted with R, v3.3.2, or GraphPad Prism, v7.02. Statistical analysis using repeated measures analysis of variance was followed by pairwise post hoc tests adjusted using the Holm method. Differences were considered significant for P values <0.05.

RESULTS

Coexpression of the ADP-A2M4 TCR and CD8α Coreceptor Enhanced CD4$^+$ T-Cell Activation

To investigate whether coexpression of the CD8α coreceptor with the affinity-enhanced MAGE-A4 TCR (ADP-A2M4CD8) would improve CD4$^+$ T-cell function, we analyzed cell surface expression of CD40L by flow cytometry as a measure of T-cell activation following antigen recognition. CD4$^+$ T-cell activation in response to MAGE-A4$^+$ A375 or MAGE-A4$^-$ Colo205 tumor cells was compared between ADP-A2M4CD8 and ADP-A2M4 (TCR only) (Fig. 1).

The percentage of CD40L$^+$ cells within the TCR$^+$ fraction of CD4$^+$ ADP-A2M4 T cells was 16.6% following exposure to MAGE-A4$^-$ Colo205, increasing to 40.1% following coculture with MAGE-A4$^+$ A375 tumor cells. A significantly higher proportion of CD4$^+$CD40L$^+$ T cells (80.2%; $P < 0.0001$) was detected within the TCR$^+$ population of ADP-A2M4CD8 T cells following recognition of MAGE-A4$^+$ A375 cells (summary data in Fig. 1A, representative plots in Fig. 1B).

Antigen-dependent T-cell proliferation was also assessed, but although both CD4$^+$ and CD8$^+$ TCR$^+$ T cells clearly proliferated in response to MAGE-A4$^+$ A375 cells compared with MAGE-A4$^-$ Colo205 cells, no significant differences were observed between ADP-A2M4 and ADP-A2M4CD8 transduced T cells across 4 donors (Supplemental Fig. 4, Supplemental Digital Content 1, http://links.lww.com/JIT/A706).

Activation of Both DCs and ADP-A2M4CD8 T Cells Was Increased When They Were Cocultured With MAGE-A4$^+$ Tumor Cells

Because enhanced CD4$^+$ T-cell activation in response to antigen was seen with engineered T cells expressing CD8α, we investigated T cell–DC interactions, an important component in effective antitumor response generation.

To investigate the effect of antigen-activated, CD8α-expressing CD4$^+$ T cells (ADP-A2M4CD8) on DC activation, maturation, and licensing, a model was developed in which immature DCs, tumor cells, and T cells were cocultured, and the release of cytokines, chemokines, and growth factors was analyzed in supernatants. We aimed to assess whether ADP-A2M4CD8 T cells would drive immature DC maturation in response to MAGE-A4–expressing tumor cells and whether DC maturation would sufficiently enhance both CD4$^+$ and CD8$^+$ T-cell antigen-specific responses. Immature DCs (CD1a$^+$CD14$^-$) generated from CD14$^+$ cells were cocultured with tumor cells (MAGE-A4$^+$ A375, NCI-H1755, and MAGE-A4$^-$ Nalm6) and ntd, ADP-A2M4, or ADP-A2M4CD8 T cells (either unseparated or purified as CD4$^+$ or CD8$^+$ T cells). In initial experiments, cells were harvested for analysis by flow cytometry, where DC maturation was confirmed by a marked upregulation of CD40 and CD80 surface expression (CD80^{high}, CD40^{high}; Fig. 2). There was no difference between unseparated ADP-A2M4CD8 and ADP-A2M4 as there was already maximal expression on DCs cocultured with ADP-A2M4. Overall, the expression of both CD40 and CD80 was lower when the DCs were cultured with isolated CD4$^+$ T cells compared with unseparated T cells. However, both markers did appear to be slightly elevated (albeit not statistically significant) when DCs were cocultured with next-generation CD4$^+$ ADP-A2M4CD8 T cells, as opposed to CD4$^+$ ADP-A2M4 T cells.

In subsequent experiments, culture supernatants were taken after 48 hours for cytokine analysis (Fig. 3; Supplemental Fig. 6, Supplemental Digital Content 1, http://links.lww.com/JIT/A706). IL-12 is typically secreted by activated DCs along with other cell types. In cocultures containing A375 or NCI-H1755 (MAGE-A4$^+$) cells, DCs, and unseparated T cells, IL-12 secretion was significantly higher in the presence of ADP-A2M4CD8 T cells compared with ADP-A2M4 T cells. Comparing cocultures containing isolated CD4$^+$ T cells, we observed higher IL-12 levels in ADP-A2M4CD8 conditions compared with ADP-A2M4 conditions (Fig. 3A). Furthermore, a chemokine involved in T-cell recruitment, MIG, was detected in all cocultures containing DCs and MAGE-A4$^+$ tumor cells. Secretion levels in conditions containing unseparated T cells or purified CD8$^+$ cells approached the limits of detection for the

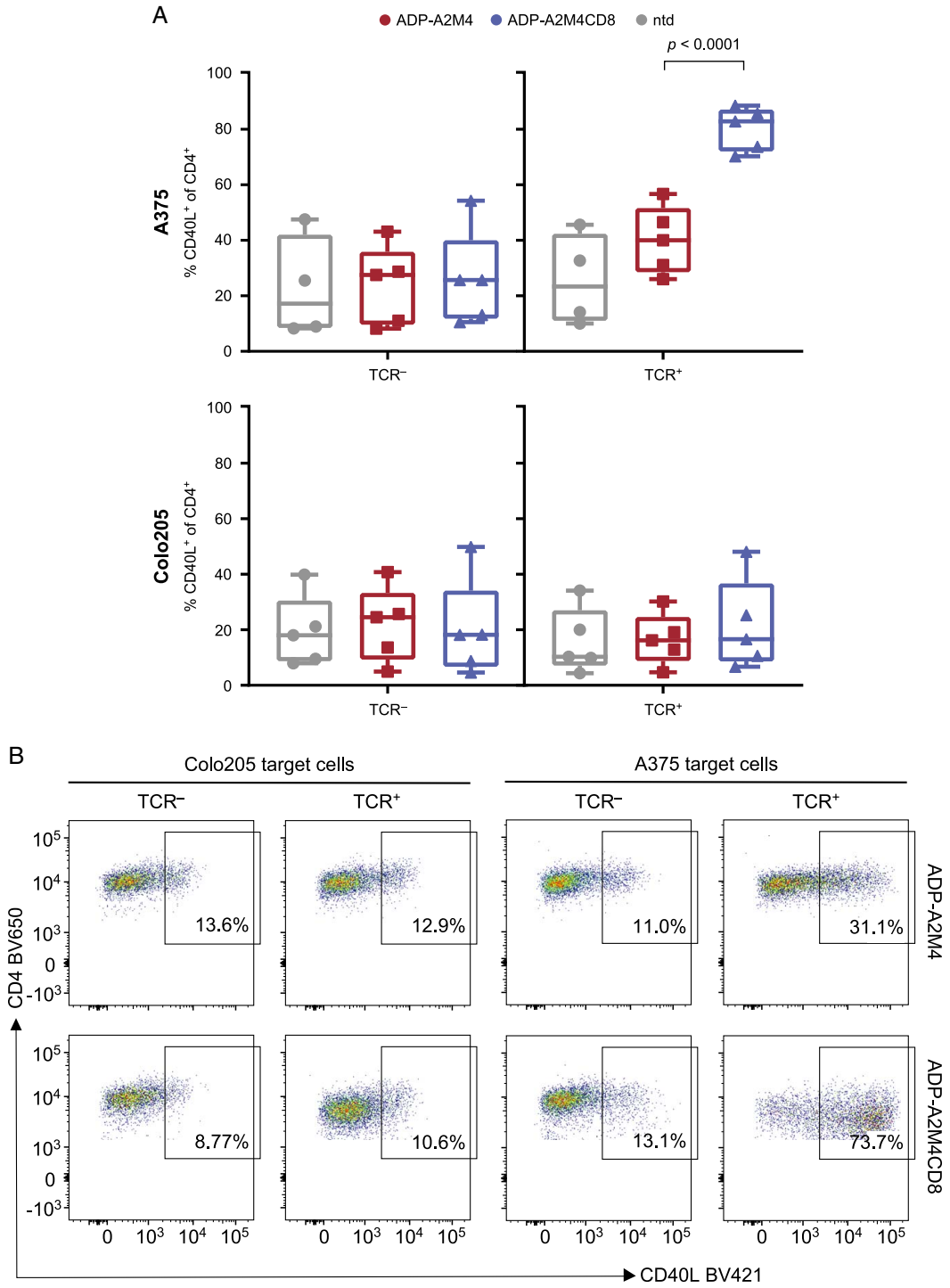

FIGURE 1. The frequency of CD40L+ cells was increased within the CD4+ subset of ADP-A2M4CD8 T cells. A, The frequency of CD40L+ T cells was determined in the TCR− and TCR+ subsets of the CD4+ T-cell population in response to stimulation with MAGE-A4+ target cells (A375; top panel) or MAGE-A4− target cells (Colo205; lower panel). Box and whisker plots summarize the data for all 5 large-scale products tested; within these, each individual data point represents one donor product (blue = ADP-A2M4CD8, red = ADP-A2M4, gray = ntd T cells). Statistical significance was assessed using a 3-way repeated measures analysis of variance, followed by pairwise post hoc tests, and *P* values were adjusted using the Holm method. B, Representative flow cytometry plots from one T-cell donor for CD4+ and TCR+/TCR− A2M4CD8 and ADP-A2M4 T cells stimulated with MAGE-A4− or MAGE-A4+ target cells. MAGE-A4 indicates melanoma-associated antigen A4; ntd, nontransduced; TCR, T-cell receptor.

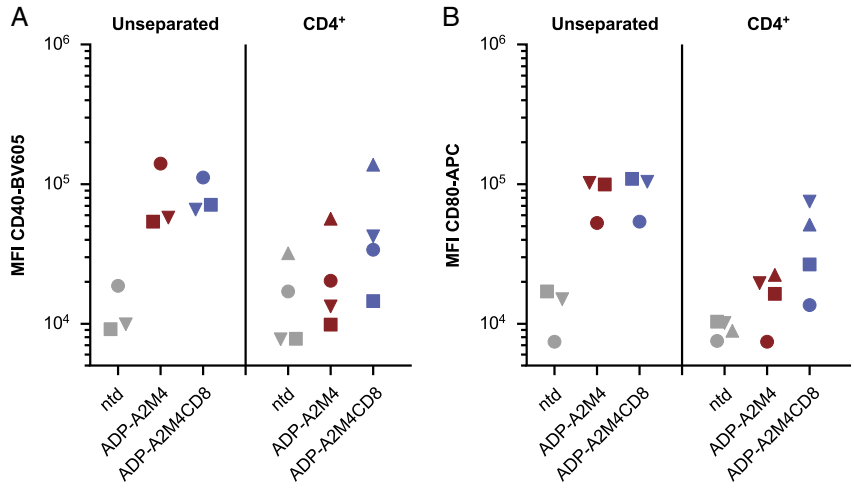

FIGURE 2. Activation of dendritic cells in coculture with T cells and MAGE-A4–expressing tumor cells. Cells were gated by surface marker CD40$^+$ (A) or CD80$^+$ (B) expression to assess the MFI. Each shape represents one T-cell batch. MAGE-A4 indicates melanoma-associated antigen A4; MFI, median fluorescence intensity; ntd, nontransduced.

assay, but in the cocultures containing purified CD4$^+$ cells, a significant difference was seen between cultures containing ADP-A2M4 or ADP-A2M4CD8 (Supplemental Fig. 6, Supplemental Digital Content 1, http://links.lww.com/JIT/A706).

Supernatants were also analyzed for cytokines associated with CD4$^+$ T-cell helper function. In cocultures containing MAGE-A4$^+$ target cells, significantly higher IFN-γ concentrations were detected with ADP-A2M4CD8 than with ADP-A2M4 T cells (Fig. 3B). Levels of IL-2 also appeared elevated in the presence of ADP-A2M4CD8 T cells over ADP-A2M4, albeit not statistically significantly (Fig. 3C). Activating naïve CD4$^+$ T cells in the presence of IFN-γ and IL-12 promotes differentiation into type 1 T-helper (Th1) cells, which in turn supports IFN-γ production and increased cytotoxic activity of CD8$^+$ T cells,[29–31] as well as further facilitating CD4$^+$ T cell–DC costimulation. Modest increases in GM-CSF, macrophage inflammatory protein-1β, and TNF-α were detected in cocultures with ADP-A2M4CD8 compared with ADP-A2M4 (Supplemental Fig. 6, Supplemental Digital Content 1, http://links.lww.com/JIT/A706).

No IL-4 secretion was detected in any cocultures, which indicates the absence of classic type 2 T-helper (Th2) cell activation (Supplemental Fig. 6, Supplemental Digital Content 1, http://links.lww.com/JIT/A706), and low levels of IL-17 were detected in all conditions. We observed moderate increases in IL-5 and IL-13 release in cultures containing ADP-A2M4CD8 compared with ADP-A2M4 cells (Supplemental Fig. 6, Supplemental Digital Content 1, http://links.lww.com/JIT/A706) and a statistically significant increase in IL-10 release in response to NCI-H1755 target cells. Opposing roles for these Th2 cytokines on tumor progression have been reported, but IL-10 and IL-13 in particular may favor tumor progression.[32,33] Importantly, in our study the presence of elevated IL-5, IL-10, and IL-13 did not affect tumor cell killing, and cytokines secreted by ADP-A2M4CD8 were also secreted to some degree by ADP-A2M4, which indicates there was no shift in the overall cytokine profile.

Taken together, these data indicate that coexpression of CD8α in CD4$^+$ T cells enhances the cytokine/chemokine landscape within T cell–DC interactions, which potentially favors a more potent DC activation and T-cell response.

ADP-A2M4CD8 CD4$^+$ T Cells Displayed Enhanced Cytotoxic Activity Against 3D Tumor Spheroids

After observing greater CD4$^+$ T-cell activation and enhanced T cell–DC interactions, we investigated whether CD4$^+$ T cells expressing ADP-A2M4CD8 would display enhanced cytotoxicity compared with ADP-A2M4 against MAGE-A4$^+$ GFP-labeled A375 tumor cells in a 3D culture model. Two sizes of microtissue were tested to assess the ability of the T cells to infiltrate and kill target cells in a more physiological setting with multiple cell-to-cell contacts rather than cells adhering to plastic. Data from the larger size are shown in Figure 4, with summary of both sizes in Supplemental Figure 7 (Supplemental Digital Content 1, http://links.lww.com/JIT/A706).

Due to the potent and rapid cytotoxic response, no significant difference in the rate of killing was seen between ADP-A2M4 and ADP-A2M4CD8, either from unseparated or purified CD8$^+$ T cells. This was not unexpected for the unseparated population as the data from purified cells illustrate that the CD8$^+$ cells kill faster than CD4$^+$ cells, and the T-cell products used in this study were generally $\geq$50% CD8$^+$ (Supplemental Fig. 1, Supplemental Digital Content 1, http://links.lww.com/JIT/A706). In contrast, with purified CD4$^+$ T cells, which generally exhibited reduced cytotoxic activity in our 3D model compared with CD8$^+$ T cells, CD4$^+$ ADP-A2M4CD8 elicited significantly higher cytotoxicity against A375.GFP spheroids compared with CD4$^+$ T cells transduced with the TCR alone ($P < 0.0001$; Figs. 4A–C; Supplemental Fig. 7, Supplemental Digital Content 1, http://links.lww.com/JIT/A706; Supplemental Video, Supplemental Digital Content 2. http://links.lww.com/JIT/A707). Compared with CD8$^+$ or unseparated populations, the ADP-A2M4CD8 CD4$^+$ cells showed delayed killing kinetics and required more T cells (80,000/well vs. 20,000/well) to achieve full lysis of the microtissue. This increased cytotoxicity was accompanied by a significant increase in both IFN-γ ($P < 0.001$) and GzB ($P < 0.0001$) secretion by transduced CD4$^+$ T cells that coexpressed CD8α

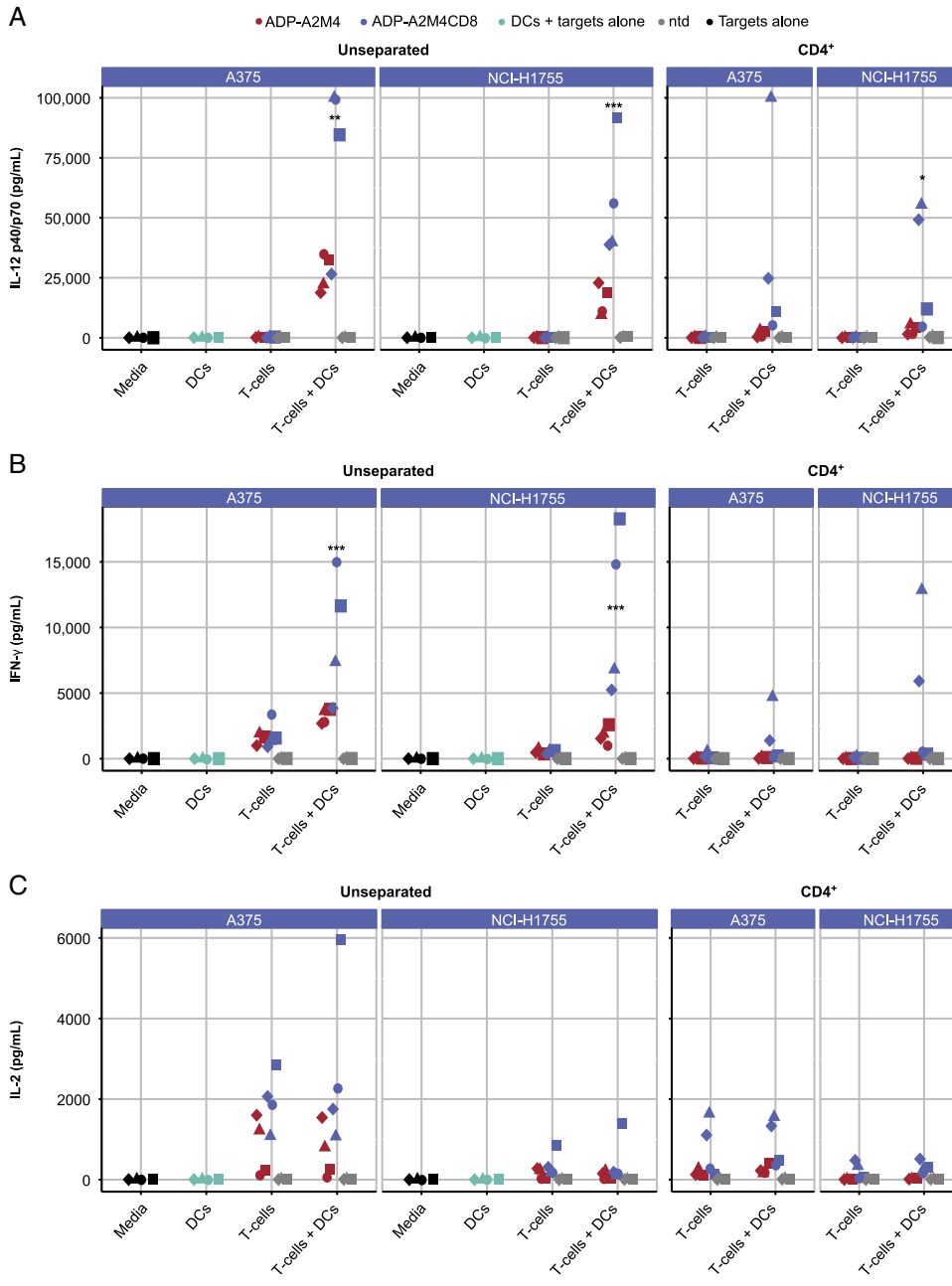

FIGURE 3. IL-12 (A), IFN-γ (B), and IL-2 (C) levels were increased in DC/tumor cell cocultures with ADP-A2M4CD8 T cells. MAGE-A4$^+$ (A375) tumor cell lines were cocultured in a 48-well plate with immature DCs and ntd T cells (gray), ADP-A2M4 (red; TCR only), or ADP-A2M4CD8 T cells (blue; TCR and CD8α). Data for additional conditions with tumor cell lines alone (black) or DCs plus tumor cells in the absence of T cells (teal) are also shown. Culture supernatants were harvested after 48 hours, and soluble mediators were analyzed by Bio-Plex MAGPIX (Bio-Rad Laboratories). Each dot represents one donor. A 3-way repeated measures analysis of variance was run for each cytokine and positive-control target, with transduction, T-cell fraction, and presence or absence of DCs as within-subject factors, followed by pairwise post hoc tests for each combination, and *P* values were adjusted using the Holm method. *$P < 0.05$; **$P < 0.01$; ***$P < 0.005$. An extended dataset can be found in Supplemental Figure 6 (Supplemental Digital Content 1, http://links.lww.com/JIT/A706). DC indicates dendritic cell; IFN-γ, interferon-gamma; IL, interleukin; MAGE-A4, melanoma-associated antigen A4; ntd, nontransduced; TCR, T-cell receptor.

(Fig. 4D). These data demonstrate that expression of the CD8α coreceptor significantly enhances the cytotoxic effector function of CD4$^+$ T cells transduced with the ADP-A2M4 TCR.

Addition of the CD8 Coreceptor Did Not Affect Specificity of the ADP-A2M4 TCR

The specificity of the ADP-A2M4 TCR has been extensively defined previously.[27] We built upon the previous

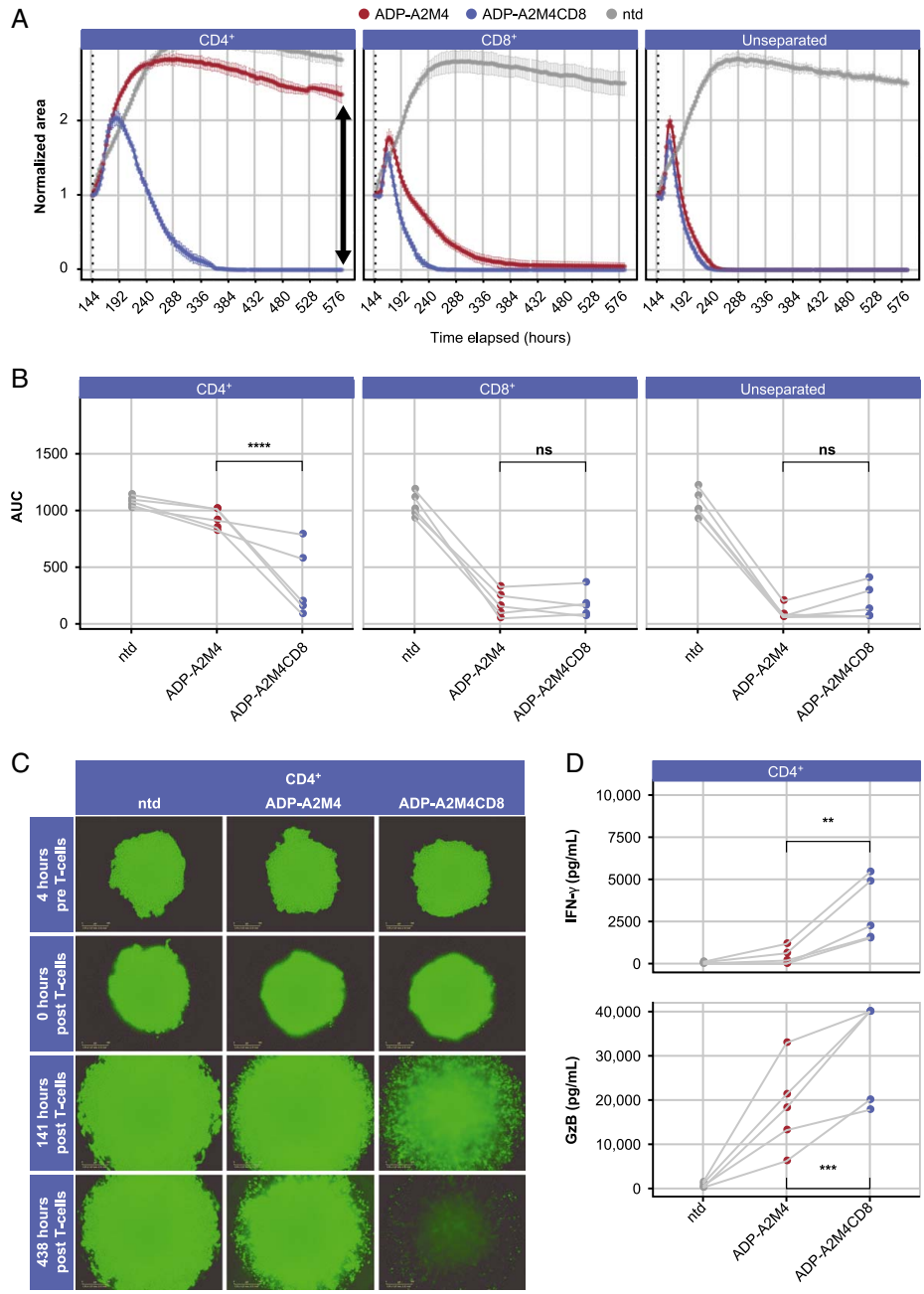

FIGURE 4. Cytotoxic activity against MAGE-A4$^+$ spheroids is enhanced with ADP-A2M4CD8 T cells. Three-dimensional spheroids of MAGE-A4$^+$ A375 melanoma cells expressing cytoplasmic GFP (A375.GFP) were treated with ADP-A2M4 (red), ADP-A2M4CD8 (blue), or ntd (gray) T cells. A, The GFP$^+$ fluorescence area of the central core of the spheroid was plotted over time for a representative donor (mean of 6 replicate wells ± SEM shown) following addition of isolated CD4$^+$ (left panel) or CD8$^+$ (central panel) T-cell fractions, or unseparated T cells (right panel). Black arrow indicates difference in microtissue spheroid area with CD4$^+$ ADP-A2M4 or ADP-A2M4CD8 T cells at the assay endpoint. B, Scatter plots showing spheroid area under the curve with isolated CD4$^+$ (left) or CD8$^+$ (center) T-cell fractions, or unseparated T cells (right). Each data point corresponds to the mean of 6 replicate wells for each donor (n = 5 donors). A and B, All data are shown normalized to the time of T-cell addition. C, Representative images of A375.GFP fluorescent spheroids treated with isolated CD4$^+$ ntd (left), ADP-A2M4 (center), or ADP-A2M4CD8 (right) T cells. D, Levels of IFN-γ (top panel) and GzB (bottom panel) produced by isolated CD$^+$ ntd, ADP-A2M4, or ADP-A2M4CD8 T cells following ~48–50 hours of coculture with A375.GFP 3-dimensional spheroids. Each data point shows the mean of 6 replicate wells for each donor (n = 5 donors). Statistical analysis was performed using repeated measures analysis of variance. $^{**}P < 0.01$; $^{***}P < 0.001$; $^{****}P < 0.0001$. AUC indicates area under the curve; GFP, green fluorescent protein; GzB, granzyme B; IFN-γ, interferon-gamma; MAGE-A4, melanoma-associated antigen A4; ns, nonsignificant; ntd, nontransduced.

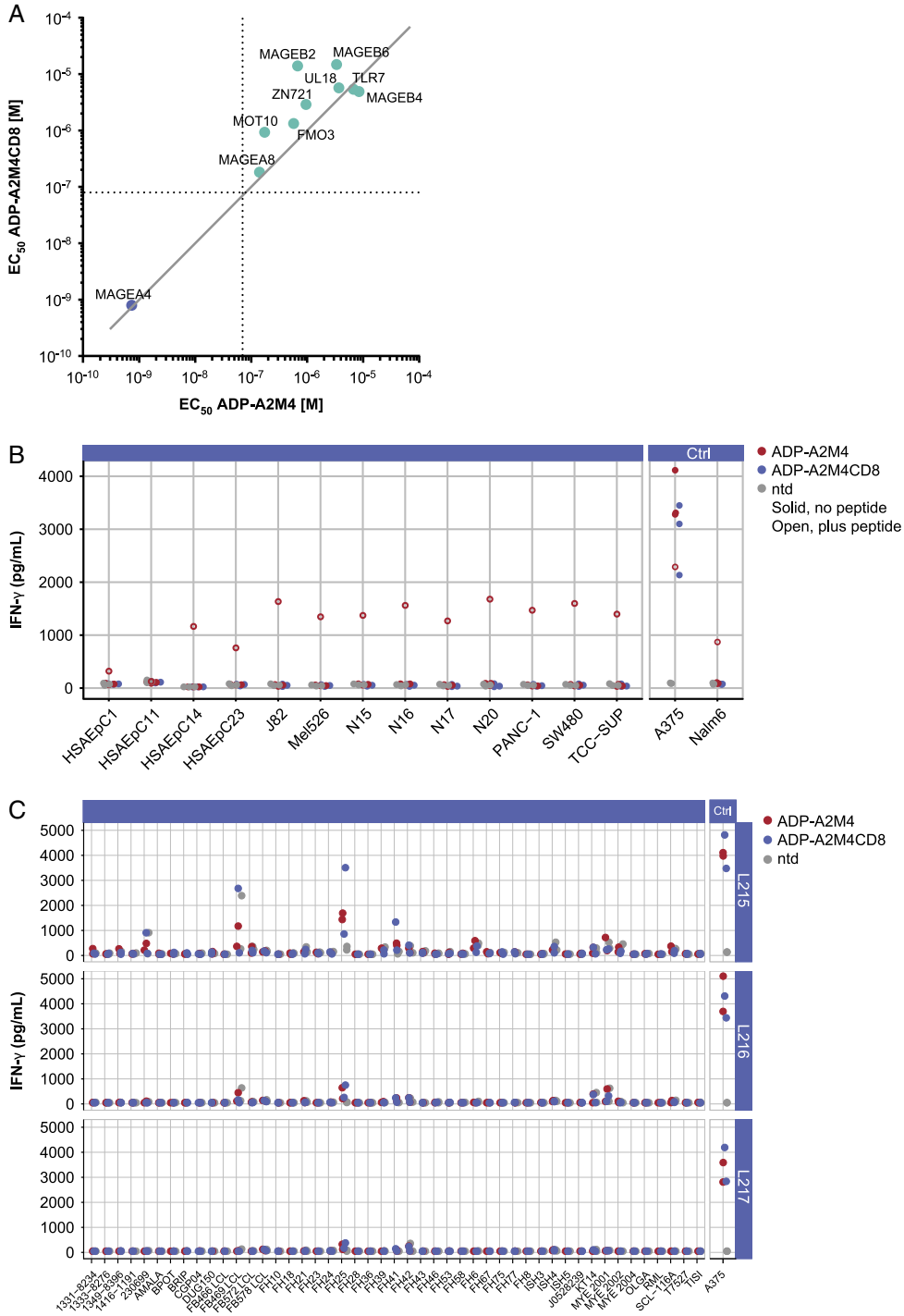

FIGURE 5. Addition of CD8α does not increase cross-reactivity of ADP-A2M4 TCR. A, Scatter plot comparison of the EC_{50} response to selected putative mimotopes and MAGE family homologous peptides for ADP-A2M4 and ADP-A2M4CD8 T cells. Data are combined geometric means from 3 T-cell products. Gray identity line indicates exact correlation, $y = x$. Dotted lines indicate 2 log shift from MAGE-$A4_{230\text{-}239}$ index peptide response from corresponding T-cell product. B, Response of ADP-A2M4 (red points), ADP-A2M4CD8 (blue points), and ntd (gray points) T cells to small airway epithelial cells (HSAEpC), melanocytes (N) or MAGE-A4$^-$ tumor cells (J82, Mel526, PANC-1, SW480, TCC-SUP), assessed by means of IFN-γ cell-based enzyme-linked immunosorbent assay. Each data point represents the mean of at least duplicate wells from a single assay. Unfilled points represent the response of ADP-A2M4 T cells against the target in the presence of 10^{-5} M MAGE-A4 peptide as a control for target cell suitability. C, IFN-γ release (pg/mL) by ntd (gray points) ADP-A2M4 (red points) and ADP-A2M4CD8 (blue points) transduced T cells after challenge with Epstein-Barr virus–derived lymphoblastoid cell line targets or MAGE-A4$^+$ A375 melanoma cells (as a positive control). Each data point represents the mean of triplicate wells in a single experiment. Data are faceted by individual T-cell preps. EC_{50} indicates half-maximal effective concentration; IFN-γ, interferon-gamma; MAGE-A4, melanoma-associated antigen A4; ntd, nontransduced.

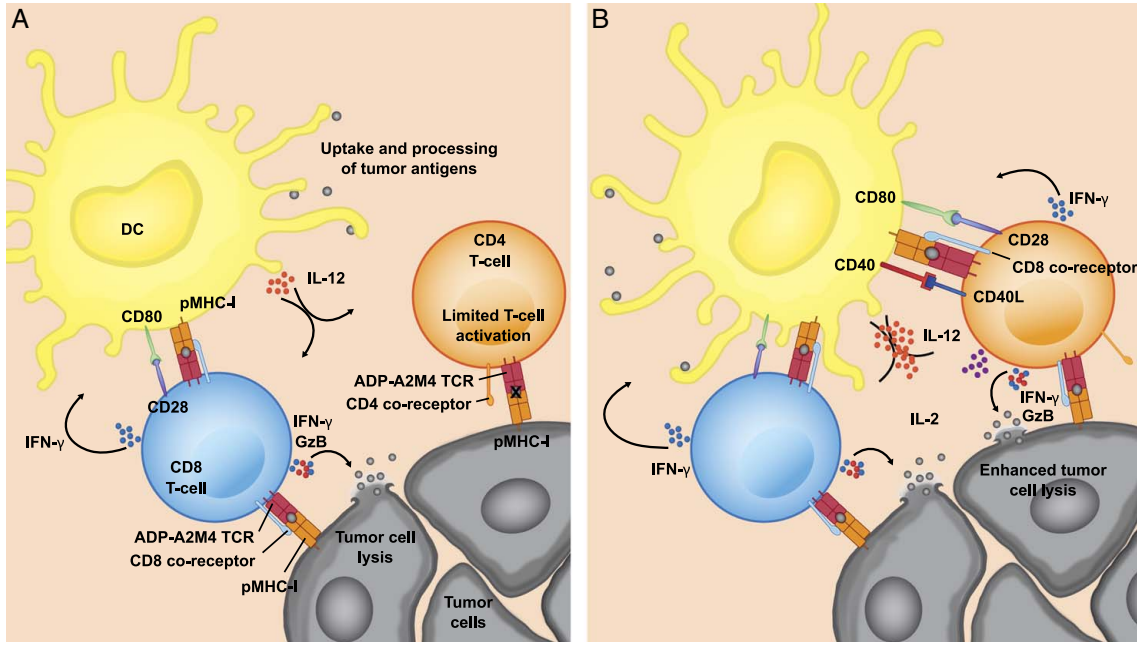

FIGURE 6. Summarized immune-cell interactions in the tumor microenvironment with engineered T cells coexpressing an affinity-enhanced TCR and CD8α. A, Tumor cells can present internal antigens to T cells via their peptide:HLA class I complex, which binds to the TCR (ADP-A2M4 TCR represented in red). $CD4^+$ T cells have a limited functional activation through the interaction with HLA class I because of the absence of the CD8 coreceptor. B, However, in ADP-A2M4CD8, the interaction between $CD4^+$ T cells and HLA class I is enhanced by the expression of CD8 coreceptors. These engineered $CD4^+$ T cells can effectively kill tumor cells, as well as stimulate DCs (eg, through CD40L/CD40 interaction), upregulate costimulatory molecules on the DC surface (eg, CD80), and induce IL-12 secretion. These mechanisms in turn boost $CD8^+$ T-cell activation, which should lead to enhanced clonal expansion and differentiation into effector and memory T cells. Therefore, ADP-A2M4CD8 is expected to enhance antitumor cytotoxic activity via improved $CD4^+$ T-cell effector and helper functions. DC indicates dendritic cell; GzB, granzyme B; IFN-γ, interferon-gamma; IL, interleukin; pMHC, peptide-loaded major histocompatibility complex; TCR, T-cell receptor.

work by retesting in a focused manner, to confirm that CD8α addition did not affect the ADP-A2M4 TCR specificity, nor enhance previously identified weak cross-reactivities.

Thirty-nine peptides previously shown to weakly activate the ADP-A2M4 TCR were tested, and those that induced T-cell responses with a sufficient magnitude to establish half-maximal effective concentration (EC_{50}) are plotted in Figure 5A. No new peptide reactivities were revealed, and the relative EC_{50} between ADP-A2M4 and ADP-A2M4CD8 cells remained close to the line of identity, indicating no qualitative or quantitative effect on TCR specificity. In Figure 5B, a small panel of cell lines representing tissue types potentially recognized by the ADP-A2M4 TCR[27] were retested, and no T-cell reactivity was seen. Finally, in Figure 5C, a panel of 47 Epstein-Barr virus–transformed lymphoblastoid cell lines representing a broad spectrum of HLA types was tested (for full typing, see Supplemental Table 2, Supplemental Digital Content 1, http://links.lww.com/JIT/A706). Reactivity above endogenous levels seen with ntd T cells was observed with 2 HLA-A*02:05 cell lines (FH25 and FH41), which is a previously defined ADP-A2M4 TCR alloreactivity. In cases where reactivity was seen with ntd and TCR-transduced T cells, the lymphoblastoid cell line shared an HLA allele with the T-cell donor; this is likely a response of the donor's endogenous TCR repertoire to an Epstein-Barr virus antigen, and as such, would not be expected to be an additional risk for an autologous therapy. No novel alloreactivities were observed for ADP-A2M4CD8. Overall, no increased cross-reactivity was seen with addition of CD8α to ADP-A2M4.

DISCUSSION

We tested a next-generation SPEAR T-cell product that coexpresses a CD8α coreceptor in addition to an affinity-enhanced TCR to target MAGE-A4–expressing tumors. Autologous TCR-engineered T-cell products are typically composed of both $CD8^+$ and $CD4^+$ T cells in varying proportions, which are partly dictated by the starting frequency of $CD4^+$ and $CD8^+$ T cells in the donor's peripheral blood and the expansion capability of the T cells. Although $CD4^+$ T cells may naturally have lower cytotoxic capability than $CD8^+$ T cells, they play a vital role in antitumor immune responses and act synergistically with $CD8^+$ T cells.[7–9] Most affinity-enhanced TCRs identified for use in T-cell therapy, including ADP-A2M4, are MHC class I restricted. Although transduced $CD4^+$ T cells can respond through an MHC class I–restricted TCR (some response from $CD4^+$ ADP-A2M4 T cells in the present study, also see Tan et al[26]), full TCR activation may not occur without stabilization of pMHC-TCR interactions by CD8.[34] This may impede a potent cytotoxic $CD4^+$ T-cell antitumor response in a TCR-only product (Fig. 6A). Engineering $CD4^+$ T cells to coexpress a CD8α coreceptor alongside an affinity-enhanced MHC class I–restricted TCR was expected to boost both $CD4^+$ T-cell helper and effector functions (Fig. 6B).

Our data confirm that CD8α coreceptor expression leads to increased upregulation of CD40L on TCR-transduced CD4+ T cells upon recognition of MAGE-A4+ target cells when compared with T cells transduced with the TCR alone. This can lead to increased stimulation of DCs via interaction with CD40, which is elevated on the surface of the DCs along with CD80 (another costimulatory molecule) and induces the secretion of IL-12. As anticipated, these mechanisms appeared to boost T-cell activation, with ADP-A2M4CD8 T cells producing more IFN-γ, IL-2, and GzB than ADP-A2M4 T cells. CD4+ ADP-A2M4CD8 T cells also displayed more potent cytotoxic responses against an in vitro 3D tumor model. The increased potency against MAGE-A4+ targets does not result in detrimental changes in T-cell specificity.

Two studies took a similar approach, in which TCRs against MAGE-A1[35] or gp100[36] were coexpressed alongside a CD8α coreceptor, with significant improvements observed in Th1 cytokine release and cytotoxicity. Furthermore, a CD8αβ coreceptor was expressed alongside an antiviral TCR showing increased functional avidity of the TCR in human CD4+ T cells, increased cytokine production and cytotoxicity in vitro, and increased in vivo antitumor efficacy in an adoptive transfer setting.[37] These studies support our work, as we observed improved CD4+ T-cell activation for ADP-A2M4CD8 in response to antigen compared with T cells transduced with the TCR alone and an upregulation in Th1 cytokine secretion (ie, IFN-γ, IL-2). We did not see improved proliferation in CD4+ ADP-A2M4CD8 compared with CD4+ ADP-A2M4 cells. However, CD4+ ADP-A2M4 T cells already proliferate in response to antigen to almost the same extent as CD8+ cells (Supplemental Fig. 4, Supplemental Digital Content 1, http://links.lww.com/JIT/A706), which is not the case for every TCR,[38] so there is limited scope for improvement within the confines of this assay.

Previous studies with both human and mouse T cells[39–41] suggested that CD4+ T cells expressing CD8αβ displayed enhanced CD4+ function compared with CD4+ T cells expressing CD8α only. Although we have not directly compared coexpression of CD8αβ versus CD8α in this study, our data demonstrate that expression of CD8α coreceptor led to an improvement in CD4+ T-cell function across multiple assays. Neither upregulated CD40L expression nor increased IFN-γ secretion by CD8α-transduced MHC class I–specific CD4+ T cells in mice were observed by Kessels et al,[41] yet we saw these improvements with our human TCR in this study. Therefore, any possible benefit of CD8αβ over CD8α alone may depend on the species, manufacturing protocol, TCR affinity, or other intrinsic factors unique to each individual TCR. Furthermore, taking the CD8α and TCR coexpression approach has benefits compared with CD8αβ regarding vector size, because larger lentiviral vectors are known to have reduced effective viral titer, resulting in lower transduction efficiency.[42]

One potential effect of coexpressing the CD8 coreceptor in CD4+ T cells is that the cytokine production CD4+ T-helper profile may be altered. Willemsen et al[36] saw a favorable shift in the cytokine profile of CD4+ T cells coexpressing the CD8α coreceptor, reporting increased Th1 and decreased Th2 cytokine production, whereas Xue et al[37] reported no change in the cytokine profile of CD4+ T cells with the addition of CD8αβ, only an increase in cytokine production magnitude. Our data reflect the latter case, with an increase in magnitude of response but no significant shift in overall profile.

T cells do not work in isolation, and an antitumor response requires coordination of many facets of the immune system. DCs comprise one key cell type in coordinating the local immune response. Adoptive T cells failed to control tumors lacking resident CD103+ DCs, owing to an inability of effector and memory T cells to be recruited to the tumor site.[43] Another report[44] suggests that immune checkpoint inhibitor efficacy depends on the crosstalk between T cells and tumor-resident DCs and involves IL-12 and IFN-γ. Furthermore, it is known that cancer-tolerogenic immature or semi-mature tumor-infiltrating DCs require additional stimuli to fully mature and drive a proper immune response that includes T-cell priming, licensing, support, and antigen spread.[45] Therefore, we assessed the effect of coexpression of CD8α in CD4+ T cells in a 3-way coculture (Fig. 6) with a focus on the secretion of soluble inflammatory mediators by both DCs and T cells. In this model, we saw significantly higher levels of IL-12 and IFN-γ and moderately elevated GM-CSF, TNF-α, IL-5, and IL-13 with CD4+ ADP-A2M4CD8 T cells compared with a coculture with CD4+ ADP-A2M4 T cells. This suggests the potential for an enhanced inflammatory milieu within tumors exposed to ADP-A2M4CD8. In addition, there is the potential for activated DCs to prime endogenous tumor-specific T cells more effectively, leading to their expansion and resulting in epitope spreading, possibly engaging other inflammatory immune players, as recently illustrated.[46] Broadening the immune response may also reduce the chance for the formation of tumor-immune escape variants through expansion of the T-cell response to multiple epitopes at once.

CD4+ T cells play a key support role, although cytotoxic activity has also been observed.[10–12,47–49] In the present study, a significant enhancement in direct CD4+ T-cell cytotoxic activity against MAGE-A4+ tumor cells was seen with CD4+ ADP-A2M4CD8 T cells, demonstrating that coexpression of CD8α alongside the TCR provides additional cytotoxic benefits that contribute to tumor control in addition to the enhanced CD4+ helper functions (Fig. 6B). Naturally occurring CD4 cytotoxic cells have been characterized in antiviral immunity[50] and an antitumor context.[51] These CD4 cytotoxic T lymphocytes share characteristics with Th1 cells (secreting IFN-γ, IL-2, and TNF-α) and kill through a granzyme/perforin-dependent pathway with delayed kinetics compared with CD8+ cells. When cytotoxic activity is induced in CD4+ cells through either expression of an introduced chimeric antigen receptor[52] or coincubation with tumor-targeting bispecific antibody,[53] similar behavior is seen. This behavior holds true for ADP-A2M4CD8 cells with robust but slightly delayed killing of 3D microtissues alongside the secretion of GzB and IFN-γ.

Taken together, our data support the benefit of adding CD8α to TCR-engineered T cells as this provides enhanced CD4+ T-helper and cytotoxic functions and may improve long-term T-cell function such as memory formation of both CD4 and CD8 subsets, change the tumor microenvironment, and lead to more potent and durable antitumor responses in vivo. While similar approaches in human cells have been published,[35–38] this study adds data from an additional, clinical-stage TCR and is the first extensive study of the effect of CD8 on the specificity of the resulting engineered T cells. In addition, ADP-A2M4CD8 was the first next-generation engineered TCR therapy using CD8 to progress to the clinic. The SURPASS trial opened in 2019 and is a phase 1, open-label, dose-escalation clinical trial (NCT04044859) with

promising preliminary results in multiple tumor types,[54,55] supporting the opening of a phase 2 trial in advanced esophageal or esophagogastric junction cancers in 2021 (NCT04752358).

ACKNOWLEDGMENTS

The authors acknowledge and thank their colleagues in protein sciences (Ellen Border, Bartosz Muszynski, Aleksandra Dziewulska, and Jana Rundle) for the cloning and production of the TCR plasmids. They also thank the blood donors.

Louise V. Rice died in November 2019, before the completion of the manuscript. A.M.W., A.B.G., A.S., B.L., C.G., J.D.S, L.M., R.J.M.A., R.Y.D., S.D., and T.A. were affiliated with Adaptimmune at the time the study was conducted.

CONFLICTS OF INTEREST/FINANCIAL DISCLOSURES

This study was sponsored by Adaptimmune. Editorial support for this manuscript was provided by Elevate Scientific Solutions (Envision Pharma Group), which was contracted and compensated by Adaptimmune for these services.

All authors were employees of Adaptimmune at the time of the study and may own stock/stock options in Adaptimmune. B.L. is a full-time employee of Laboratoires Servier.

REFERENCES

1. Martinez M, Moon EK. CAR T cells for solid tumors: new strategies for finding, infiltrating, and surviving in the tumor microenvironment. *Front Immunol*. 2019;10:128.
2. D'Angelo SP, Melchiori L, Merchant MS, et al. Antitumor activity associated with prolonged persistence of adoptively transferred NY-ESO-1^{c259} T cells in synovial sarcoma. *Cancer Discov*. 2018;8:944–957.
3. Robbins PF, Morgan RA, Feldman SA, et al. Tumor regression in patients with metastatic synovial cell sarcoma and melanoma using genetically engineered lymphocytes reactive with NY-ESO-1. *J Clin Oncol*. 2011;29:917–924.
4. D'Angelo SP, Araujo DM, Van Tine BA, , et al. Comparison of pre-treatment conditioning on efficacy in two cohorts of a pilot study of genetically engineered NY-ESO-1^{c259} T cells in patients with synovial sarcoma. Presented at Fourth CRI-CIMT-EATI-AACR International Cancer Immunotherapy Conference, New York, NY; 2018.
5. Robbins PF, Kassim SH, Tran TL, et al. A pilot trial using lymphocytes genetically engineered with an NY-ESO-1-reactive T-cell receptor: long-term follow-up and correlates with response. *Clin Cancer Res*. 2015;21:1019–1027.
6. Stadtmauer EA, Faitg TH, Lowther DE, et al. Long-term safety and activity of NY-ESO-1 SPEAR T cells after autologous stem cell transplant for myeloma. *Blood Adv*. 2019;3:2022–2034.
7. Ostroumov D, Fekete-Drimusz N, Saborowski M, et al. CD4 and CD8 T lymphocyte interplay in controlling tumor growth. *Cell Mol Life Sci*. 2018;75:689–713.
8. Borst J, Ahrends T, Babala N, et al. CD4$^+$ T cell help in cancer immunology and immunotherapy. *Nat Rev Immunol*. 2018;18:635–647.
9. Ahrends T, Borst J. The opposing roles of CD4$^+$ T cells in anti-tumour immunity. *Immunology*. 2018;154:582–592.
10. Quezada SA, Simpson TR, Peggs KS, et al. Tumor-reactive CD4$^+$ T cells develop cytotoxic activity and eradicate large established melanoma after transfer into lymphopenic hosts. *J Exp Med*. 2010;207:637–650.
11. Veatch JR, Lee SM, Fitzgibbon M, et al. Tumor-infiltrating BRAFV600E-specific CD4+ T cells correlated with complete clinical response in melanoma. *J Clin Invest*. 2018;128:1563–1568.
12. Hunder NN, Wallen H, Cao J, et al. Treatment of metastatic melanoma with autologous CD4+ T cells against NY-ESO-1. *N Engl J Med*. 2008;358:2698–2703.
13. Alspach E, Lussier DM, Miceli AP, et al. MHC-II neoantigens shape tumour immunity and response to immunotherapy. *Nature*. 2019;574:696–701.
14. Zuazo M, Arasanz H, Fernández-Hinojal G, et al. Functional systemic CD4 immunity is required for clinical responses to PD-L1/PD-1 blockade therapy. *EMBO Mol Med*. 2019;11:e10293.
15. Barta SK, Zain J, MacFarlane AW, et al. Phase II study of the PD-1 inhibitor pembrolizumab for the treatment of relapsed or refractory mature T-cell lymphoma. *Clin Lymphoma Myeloma Leuk*. 2019;19:356–364.
16. Melssen M, Slingluff CL Jr. Vaccines targeting helper T cells for cancer immunotherapy. *Curr Opin Immunol*. 2017;47:85–92.
17. Aldrich JF, Lowe DB, Shearer MH, et al. CD4+ T lymphocytes are critical mediators of tumor immunity to simian virus 40 large tumor antigen induced by vaccination with plasmid DNA. *J Virol*. 2011;85:7216–7224.
18. Gulley JL, Madan RA, Pachynski R, et al. Role of antigen spread and distinctive characteristics of immunotherapy in cancer treatment. *J Natl Cancer Inst*. 2017;109:djw261.
19. Sun JC, Bevan MJ. Defective CD8 T cell memory following acute infection without CD4 T cell help. *Science*. 2003;300:339–342.
20. Ahrends T, Busselaar J, Severson TM, et al. CD4$^+$ T cell help creates memory CD8$^+$ T cells with innate and help-independent recall capacities. *Nat Commun*. 2019;10:5531.
21. Li Y, Mariuzza R. Structural and biophysical insights into the role of CD4 and CD8 in T cell activation. *Front Immunol*. 2013;4:206.
22. Devine L, Sun J, Barr MR, et al. Orientation of the Ig domains of CD8 alpha beta relative to MHC class I. *J Immunol*. 1999;162:846–851.
23. Gao GF, Tormo J, Gerth UC, et al. Crystal structure of the complex between human CD8αα and HLA-A2. *Nature*. 1997;387:630–634.
24. Holler PD, Kranz DM. Quantitative analysis of the contribution of TCR/pepMHC affinity and CD8 to T cell activation. *Immunity*. 2003;18:255–264.
25. Davis MM, Krogsgaard M, Huppa JB, et al. Dynamics of cell surface molecules during T cell recognition. *Annu Rev Biochem*. 2003;72:717–742.
26. Tan MP, Dolton GM, Gerry AB, et al. Human leucocyte antigen class I-redirected anti-tumour CD4$^+$ T cells require a higher T cell receptor binding affinity for optimal activity than CD8$^+$ T cells. *Clin Exp Immunol*. 2017;187:124–137.
27. Sanderson JP, Crowley DJ, Wiedermann GE, et al. Preclinical evaluation of an affinity-enhanced MAGE-A4-specific T-cell receptor for adoptive T-cell therapy. *Oncoimmunology*. 2019;9:1682381.
28. Roederer M. Interpretation of cellular proliferation data: avoid the panglossian. *Cytometry A*. 2011;79:95–101.
29. Wang X, Wu T, Zhou F, et al. IL12p40 regulates functional development of human CD4$^+$ T cells: enlightenment by the elevated expressions of IL12p40 in patients with inflammatory bowel diseases. *Medicine*. 2015;94:e613.
30. Powell MD, Read KA, Sreekumar BK, et al. IL-12 signaling drives the differentiation and function of a T_H1-derived T_{FH1}-like cell population. *Sci Rep*. 2019;9:13991.
31. Rubinstein MP, Su EW, Suriano S, et al. Interleukin-12 enhances the function and anti-tumor activity in murine and human CD8$^+$ T cells. *Cancer Immunol Immunother*. 2015;64:539–549.
32. Terabe M, Park JM, Berzofsky JA. Role of IL-13 in regulation of anti-tumor immunity and tumor growth. *Cancer Immunol Immunother*. 2004;53:79–85.
33. Dennis KL, Blatner NR, Gounari F, et al. Current status of interleukin-10 and regulatory T-cells in cancer. *Curr Opin Oncol*. 2013;25:637–645.
34. Wooldridge L, van den Berg HA, Glick M, et al. Interaction between the CD8 coreceptor and major histocompatibility

complex class I stabilizes T cell receptor-antigen complexes at the cell surface. *J Biol Chem*. 2005;280:27491–27501.
35. Willemsen R, Ronteltap C, Heuveling M, et al. Redirecting human CD4+ T lymphocytes to the MHC class I-restricted melanoma antigen MAGE-A1 by TCR alphabeta gene transfer requires CD8alpha. *Gene Ther*. 2005;12:140–146.
36. Willemsen RA, Sebestyen Z, Ronteltap C, et al. CD8 alpha coreceptor to improve TCR gene transfer to treat melanoma: down-regulation of tumor-specific production of IL-4, IL-5, and IL-10. *J Immunol*. 2006;177:991–998.
37. Xue SA, Gao L, Ahmadi M, et al. Human MHC Class I-restricted high avidity CD4+ T cells generated by co-transfer of TCR and CD8 mediate efficient tumor rejection in vivo. *Oncoimmunology*. 2013;2:e22590.
38. Dossa RG, Cunningham T, Sommermeyer D, et al. Development of T-cell immunotherapy for hematopoietic stem cell transplantation recipients at risk of leukemia relapse. *Blood*. 2018;131:108–120.
39. Morris EC, Tsallios A, Bendle GM, et al. A critical role of T cell antigen receptor-transduced MHC class I-restricted helper T cells in tumor protection. *Proc Natl Acad Sci USA*. 2005;102:7934–7939.
40. McNicol AM, Bendle G, Holler A, et al. CD8alpha/alpha homodimers fail to function as co-receptor for a CD8-dependent TCR. *Eur J Immunol*. 2007;37:1634–1641.
41. Kessels HW, Schepers K, van den Boom MD, et al. Generation of T cell help through a MHC class I-restricted TCR. *J Immunol*. 2006;177:976–982.
42. Kumar M, Keller B, Makalou N, et al. Systematic determination of the packaging limit of lentiviral vectors. *Hum Gene Ther*. 2001;12:1893–1905.
43. Spranger S, Dai D, Horton B, et al. Tumor-residing Batf3 dendritic cells are required for effector T cell trafficking and adoptive T cell therapy. *Cancer Cell*. 2017;31:711–723.
44. Garris CS, Arlauckas SP, Kohler RH, et al. Successful anti-PD-1 cancer immunotherapy requires T cell-dendritic cell crosstalk involving the cytokines IFN-γ and IL-12. *Immunity*. 2018;49:1148–1161.
45. Dudek A, Martin S, Garg A, et al. Immature, semi-mature, and fully mature dendritic cells: toward a DC-cancer cells interface that augments anticancer immunity. *Front Immunol*. 2013;4:438.
46. Menares E, Gálvez-Cancino F, Cáceres-Morgado P, et al. Tissue-resident memory CD8+ T cells amplify anti-tumor immunity by triggering antigen spreading through dendritic cells. *Nat Commun*. 2019;10:4401.
47. Nelson MH, Knochelmann HM, Bailey SR, et al. Identification of human CD4+ T cell populations with distinct antitumor activity.. *Sci Adv*. 2020;6::eaba7443.
48. Oh DY, Kwek SS, Raju SS, et al. Intratumoral CD4+ T cells mediate anti-tumor cytotoxicity in human bladder cancer. *Cell*. 2020;181:1612–1625.
49. Takeuchi A, Saito T, CD4 CTL. a cytotoxic subset of CD4+ T cells, their differentiation and function. *Front Immunol*. 2017;8:194.
50. Phetsouphanh C, Pillai S, Zaunders JJ. Editorial: Cytotoxic CD4+ T cells in viral infections. *Front Immunol*. 2017;8:1729.
51. Cachot A, Bilous M, Liu YC, et al. Tumor-specific cytolytic CD4 T cells mediate immunity against human cancer. *Sci Adv*. 2021;7:eabe3348.
52. Wang D, Aguilar B, Starr R, et al. Glioblastoma-targeted CD4 + CAR T cells mediate superior antitumor activity. *JCI Insight*. 2018;3:e99048.
53. Feldmann A, Arndt C, Topfer K, et al. Novel humanized and highly efficient bispecific antibodies mediate killing of prostate stem cell antigen-expressing tumor cells by CD8+ and CD4+ T cells. *J Immunol*. 2012;189:3249–3259.
54. Hong D, Clarke J, Johanns T, et al. 379 Initial safety, efficacy, and product attributes from the SURPASS trial with ADP-A2M4CD8, a SPEAR T-cell therapy incorporating an affinity optimized TCR targeting MAGE-A4 and a CD8α co-receptor. *J Immunother Cancer*. 2020;8:A231–A231.
55. Hong DS, Clarke JM, Asch A, et al. 540P Safety and efficacy from the SURPASS trial with ADP-A2M4CD8, a SPEAR T-cell therapy incorporating a CD8α co-receptor and an affinity optimized TCR targeting MAGE-A4. *Ann Oncol*. 2021;32:S604–S605.

